12. Scholz, C. H., Sykes, L. R. & Aggarwal, Y. P. Earthquake prediction: a physical basis. *Science* **181,** 803–810 (1973).
13. Igarashi, G., Wakita, H. & Sato, T. Precursory and coseismic anomalies in well water levels observed for the February 2, 1992 Tokyo Bay earthquake. *Geophys. Res. Lett.* **19,** 1583–1586 (1992).
14. Roeloffs, E. A. Hydrologic precursors to earthquakes: a review. *Pure Appl. Geophys.* **126,** 177–209 (1988).
15. Muir-Wood, R. & King, G. C. P. Hydrological signatures of earthquake strain. *J. Geophys. Res.* **98,** 22035–22068 (1993).
16. Mizutani, H., Ishido, T., Yokotura, T. & Onishi, S. Electrokinetic phenomena associated with earthquakes. *Geophys. Res. Lett.* **3,** 365–368 (1976).
17. Jouniaux, L. & Pozzi, J. P. Streaming potential and permeability of saturated sandstones under triaxial stress: consequences for electrotelluric anomalies prior to earthquakes. *J. Geophys. Res.* **100,** 10197–10209 (1995).
18. Bernard, P. Plausibility of long distance electrotelluric precursors to earthquakes. *J. Geophys. Res.* **97,** 17531–17546 (1992).
19. King, C. Y. Gas geochemistry applied to earthquake prediction: an overview. *J. Geophys. Res.* **91,** 12269–12281 (1986).
20. Morat, P. & Le Mouël, J. L. Electrical signals generated by the collapse of the pillars of a gypsum quarry. *C.R. Acad. Sci.* **308,** 33–38 (1989).
21. Perrier, F. *et al.* A one-year systematic study of electrodes for long period measurement of the electric field in geophysical environments. *J. Geomagn. Geoelectr.* **49,** 1677–1696 (1997).
22. Wilkening, M. H. & Watkins, D. E. Air exchange and ^{222}Rn concentrations in the Carlsbad caverns. *Health Phys.* **31,** 139–145 (1976).
23. Direction de l'Equipement Electricité De France, Note de synthèse géologique et technique, *Barrage de Roselend, Fondation de l'Ouvrage* **1–12,** (Electricité De France, Aix-en-Provence, 1952–1962). (In French.)
24. Roeloffs, E. A. Fault stability changes induced beneath a reservoir with cyclic variations in water level. *J. Geophys. Res.* **93,** 2107–2124 (1988).
25. Perrier, F., Trique, M., Hautot, S., Avouac, J. P. & Tarits, P. Electrical variations associated with yearly lake level variations. *Geophys. Res. Lett.* **25,** 1955–1958 (1998).
26. Simpson, D. W. & Negmatullaev, S. K. Induced seismicity at Nurek Reservoir, Tadjikistan, USSR. *Bull. Seismol. Soc. Am.* **71,** 1561–1586 (1981).
27. Gupta, H. K. Induced seismicity hazard mitigation through water level manipulation at Koyna, India: a suggestion. *Bull. Seismol. Soc. Am.* **73,** 679–682 (1983).
28. Silver, P. G. & Valette-Silver, N. J. Detection of hydrothermal precursors to large Northern California earthquakes. *Science* **257,** 1363–1367 (1992).
29. Rojstaczer, S., Wolf, S. & Michel, R. Permeability enhancement in the shallow crust as a cause of earthquake-induced hydrological processes. *Nature* **373,** 237–239 (1995).
30. Petiau, G. In *Proc. of the Workshop "Electrodes"* (eds Clerc, G., Perrier, F., Petiau, G. & Menvielle, M.) (Report, Centre de Recherches Geophysiques de Garchy, 1996).

Supplementary information is available on *Nature*'s World-Wide Web site (http://www.nature.com) or as paper copy from the London editorial office of *Nature*.

Acknowledgements. We thank Y. Caristan, A. Meesters and R. Pican for support, and EDF for its water level data and access to the lakes. We also thank the members of the technical team from the Département Analyse et Surveillance de l'Environment, CEA, for their dedication in performing their work in often difficult weather conditions.

Correspondence and requests for materials should be addressed to M.T. (e-mail: trique@ldg.bruyeres.cea.fr).

Three-dimensional preservation of foot movements in Triassic theropod dinosaurs

Stephen M. Gatesy*, Kevin M. Middleton*, Farish A. Jenkins Jr† & Neil H. Shubin‡

* *Department of Ecology and Evolutionary Biology, Brown University, Providence, Rhode Island 02912, USA*
† *Department of Organismic and Evolutionary Biology, and Museum of Comparative Zoology, Harvard University, Cambridge, Massachusetts 02138, USA*
‡ *Department of Biology, University of Pennsylvania, Philadelphia, Pennsylvania 19104, USA*

Dinosaur footprints have been used extensively as biostratigraphic markers, environmental indicators, measures of faunal diversity and evidence of group behaviour[1–5]. Trackways have also been used to estimate locomotor posture, gait and speed[6–11], but most prints, being shallow impressions of a foot's plantar surface, provide little evidence of the details of limb excursion. Here we describe Late Triassic trackways from East Greenland, made by theropods walking on substrates of different consistency and sinking to variable depths, that preserve three-dimensional records of foot movement. Triassic theropod prints share many features with those of ground-dwelling birds, but also demonstrate significant functional differences in position of the hallux (digit I), foot posture and hindlimb excursion.

Dinosaur trackways are common in the Ørsted Dal Member of the uppermost Fleming Fjord Formation (Norian-Rhaetian) of Jameson Land, East Greenland[12]. These strata consist of cyclically bedded fine-grained siliciclastic and carbonate-bearing units laid down as part of a large rift lake system[13]. Although the footprints are structurally diverse, almost all appear to be members of a gradational series (Fig. 1a–f). At one extreme are clearly preserved tridactyl tracks referable to the ichnogenus *Grallator* (*Anchisauripus*)[1,14,15]. Such prints are commonly attributed to bipedal theropods[16] and preserve impressions of digital pads, claws and, in some cases, skin (Fig. 1a). At the other extreme are tetradactyl, elongate prints in which the digital impressions are smooth channels constricting to narrow slits (Fig. 1f). The apparent impression of digit III is markedly longer than those of other digits; its distal end is elevated and expanded to resemble a fumarole-like crater. A posteromedially directed imprint of digit I is always present adjacent to an impression of the metatarsus. Most of the Ørsted Dal prints are intermediate in form between these two extremes (Fig. 1b–e).

The differences between tridactyl (Fig. 1a) and tetradactyl (Fig. 1f) tracks are comparable to those that have been used to distinguish faunal constituents and define ichnotaxa[1,2]. However, two lines of evidence support the hypothesis that track variation is related to theropods traversing substrates of variable consistency, rather than to differences in foot morphology. First, some individual trackways exhibit more than one variant, although no single trackway preserves a complete gradational series. Second, guineafowl and turkeys walking on substrates of different consistencies closely duplicate the structural continuum of the Greenlandic prints (Fig. 1g–j). Whereas shallow prints on a relatively firm substrate accurately replicate the plantar form of these birds (Fig. 1g), successively deeper prints into increasingly wetter sediments record the entry of the initially splayed foot and the subsequent digital convergence as the foot is extracted (Figs 1h–j, 2a). Footprints in muds of intermediate consistency show separate entry and exit furrows for digits II and IV (Fig. 1h, i). In the deepest, wettest muds, the entire foot (with digits I–IV convergent) is extracted at the anterior end of the metatarsal-digit III furrow, raising a mound of sediment (Figs 1j, 2b). Thus, as mud hydration and penetration depth increase, bird tracks elongate because the substrate intercepts foot movements that normally occur above the surface. In the elongate Triassic footprints, the subsurface pathway of the toes disrupts sedimentary laminae, which can be seen in serial sections. These three-dimensional records confirm that, as in living birds, early Mesozoic theropods sank down and forward, and extracted the foot with convergent toes. Although evidence for slight digital approximation at the end of the stance phase has been reported from shallower tracks[17], the elongate Greenlandic tracks document complete toe convergence, which is retained as a primitive feature among birds.

Although the general correspondence between extant avian and Greenlandic trackways reflects some pedal similarities, there are important functional differences between basal theropods and birds. The hallux (digit I) in ceratosaurs, such as *Coelophysis*, is sufficiently shorter than the other digits that on firm substrates it does not contact the ground (cf. Fig. 1a, b). The hallucal metatarsal, applied as a flattened splint to the midshaft of metatarsal II (Fig. 3), bears an asymmetrical condyle that permits a range of about 70° of flexion/extension and about 25° of ab/adduction of the metatarsophalangeal joint. The single interphalangeal joint, which is uniaxial, permits only flexion/extension. Fixation of metatarsal I and the configuration of the metatarsophalangeal and interphalangeal joints preclude retroversion. No known Late Triassic–Early Jurassic theropod shows evidence of an avian-like reversed hallux (*Eoraptor*, *Herrerasaurus*, *Coelophysis*, *Syntarsus*, *Procompsognathus*, *Segisaurus*, *Dilophosaurus*[18–24]). Nonetheless, the posteromedially oriented hallucal print of some tracks, which appears superficially comparable to the impression of the posteriorly directed hallux of birds (compare

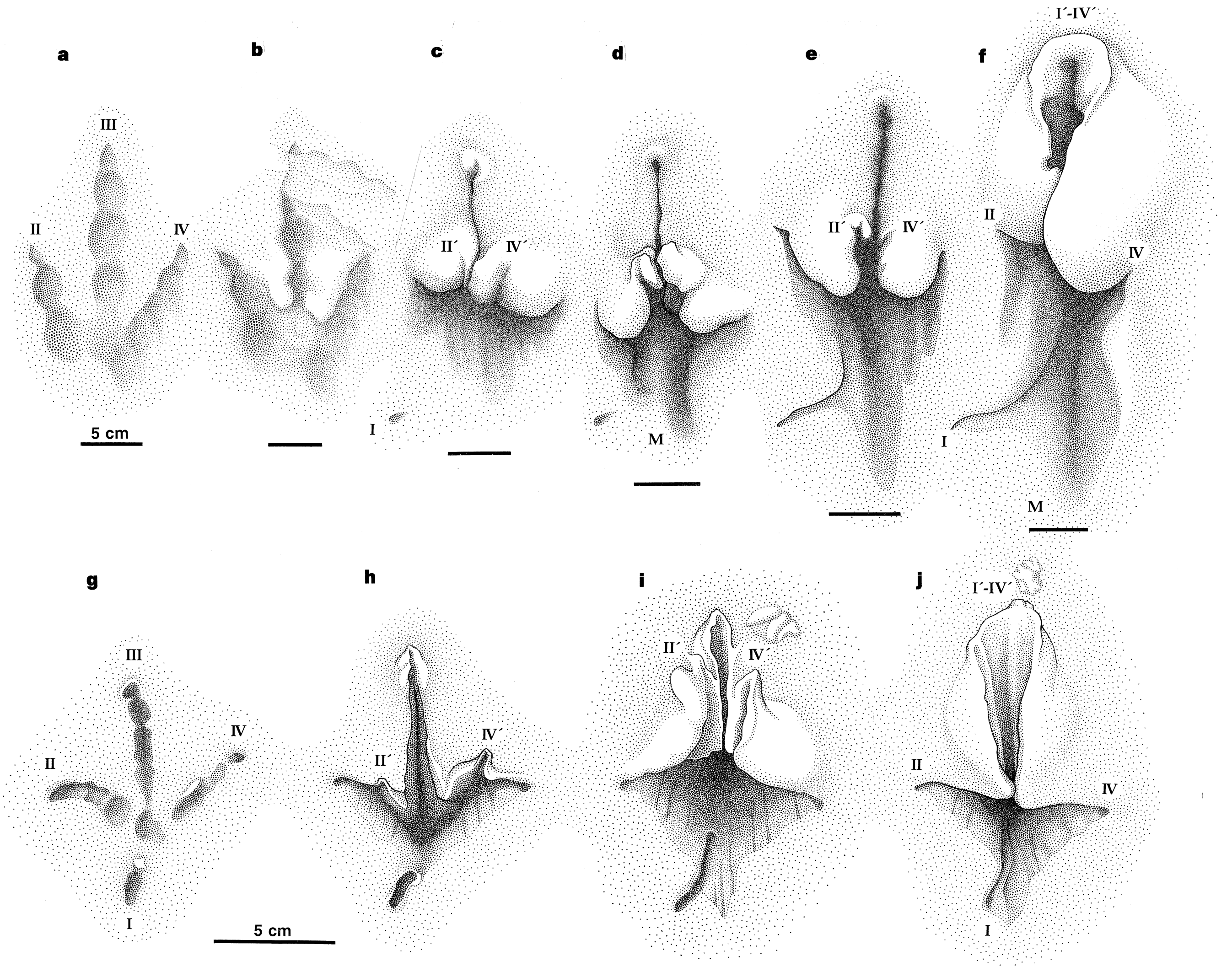

Figure 1 The spectrum of theropod tracks preserved in the Triassic Fleming Fjord Formation of Greenland (**a**–**f**) is comparable to that produced by an extant bird (the helmeted guineafowl, *Numida meleagris*) (**g**–**j**). On firm substrates, tracks closely reflect plantar morphology (**a**, **g**). The feet sink progressively deeper as sediment hydration increases (**b**–**f** and **h**–**j**). As a result, digits II and IV begin to converge before the foot is withdrawn, thereby creating separate entry (II, IV) and exit (II′, IV′) furrows (**c**–**e**, **h**, **i**) or a single terminal exit (**f**, **j**). Unlike birds, however, Triassic theropods left a distinct metatarsal impression (M) in deeper tracks (**d**–**f**). Greenlandic footprints were drawn from separate trackways and represent different individuals as well as variant details, whereas the avian prints were made by the same bird. The track illustrated in **b** is partially obscured by an overprint of another track. Theropod tracks (**a**–**f**) are registered in the Geological Museum, University of Copenhagen, as MGUH VP 3386–3391.

Fig. 1c–f and g–j), has led to speculation that undiscovered theropods with a reversed hallux existed in the early Mesozoic[2,25–27].

We propose that the Greenlandic trackways could have been created by ceratosaur feet in which the hallux was slightly abducted and flexed, but not reversed. In prints of intermediate depth, contact of the hallux with the substrate was transient, leaving an isolated mark posteromedial to the main track (Fig. 1c, d). On more pliable muds, the hallux followed the forward and downward trajectory of the foot (~45°) into the sediment. With the hallux oriented more vertically than the angle of foot penetration, an oblique impression was produced as the digit incised the surface in an anterolateral direction (Figs 1e, f, 3). Under these conditions, a foot such as that of *Coelophysis*, with an anteromedially oriented digit I, could produce a posteromedially directed hallucal furrow. Equating the hallucal entry furrow with the anatomical orientation of this digit accounts for the erroneous interpretation of a reversed hallux among early Mesozoic theropod trackmakers.

A second distinction between the Greenlandic tracks and those of living birds is the metatarsal imprint. The deepest theropod tracks are posteriorly elongated by a smooth metatarsal impression with a shallow slope of 25–30° (Fig. 1e, f). Turkeys and guineafowl, in contrast, leave little or no metatarsal print, even in the deepest tracks (Fig. 1i, j). As the avian foot penetrates down and forward, the metatarsus rapidly becomes more vertical than the angle of foot penetration, and thus no posterior metatarsal impression is created (Fig. 2b). In contrast, the distinct metatarsal imprint in Greenlandic tracks indicates that the initial foot posture was maintained during the early part of the stance phase in these theropods (Fig. 3).

The contrast between Triassic theropods and extant birds in the timing of metatarsal rotation implies differences in the movement of more proximal hindlimb segments. Among birds today, the stance phase of walking is characterized by large excursions at the knee and metatarsophalangeal joints, but little movement at the hip and ankle. During the first half of the stance phase, a relatively small femoral excursion is coupled with early elevation of the metatarsus. In contrast, walking crocodilians employ little movement at the knee and metatarsophalangeal joints; the metatarsus remains stable in early stance, when hip extension and ankle dorsiflexion predominate[28]. On the basis of caudopelvic anatomy, retraction of the femur (hip extension) has been proposed as the principal

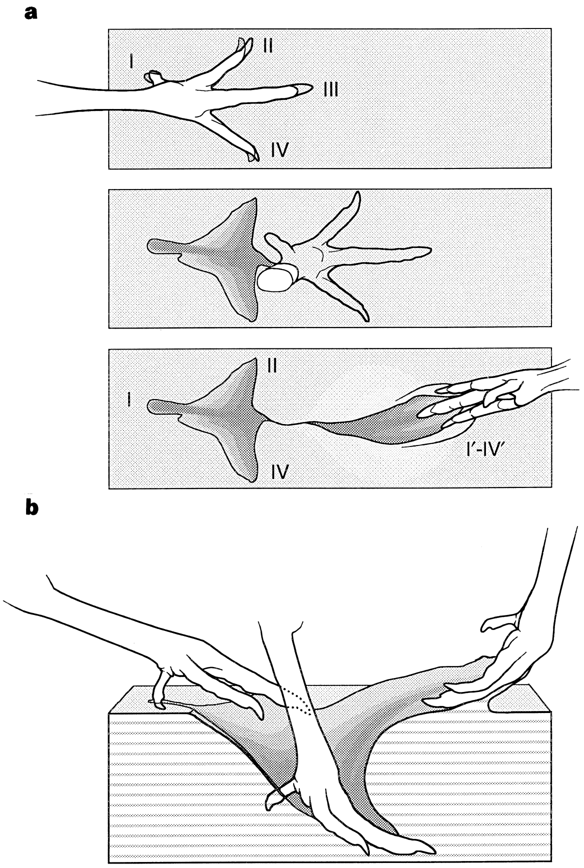

Figure 2 Early, middle, and late phases in the formation of a turkey footprint in deep mud. **a**, Dorsal and **b**, Lateral views. As the foot penetrates down and forward, the metatarsus becomes more vertical, leaving little or no impression at the rear of the track. The digits converge subsurface, emerging from the substrate (I′–IV′) well in front of their points of entry (I–IV). Foot positions were reconstructed from video records of a single stride taken simultaneously in lateral and posterior views, and aligned with respect to the resulting track.

stance-phase movement in basal theropods[29,30]. The impressions left by stable metatarsi in deep tracks from the Greenlandic Triassic are independent evidence that these theropods powered the early stance phase by femoral retraction, rather than by knee flexion as in living birds. ☐

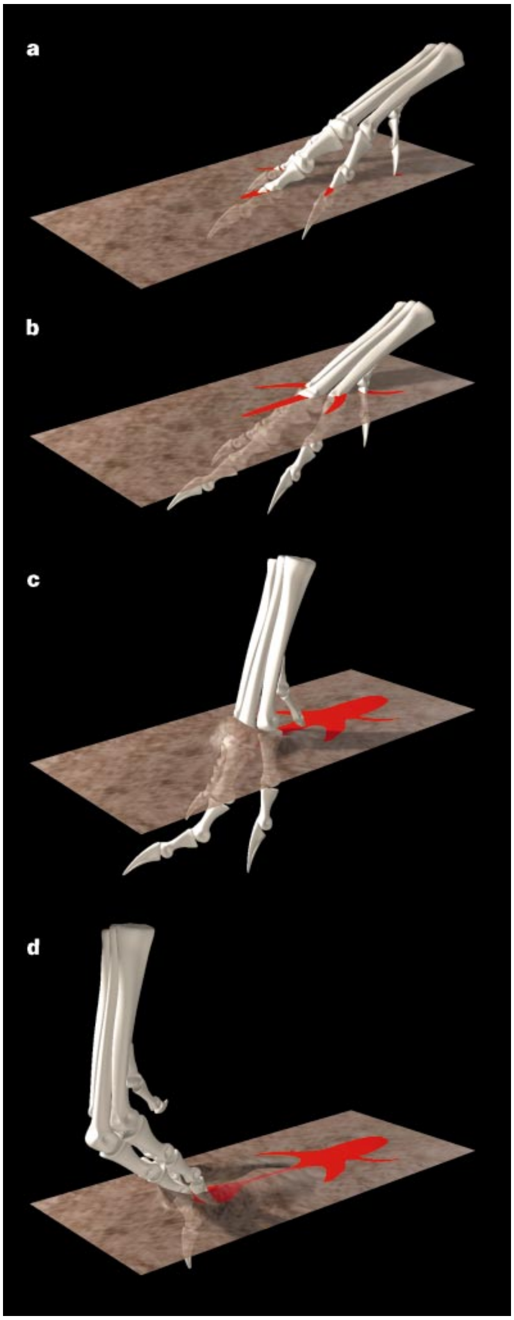

Figure 3 Three-dimensional computer reconstruction of theropod foot movements producing an elongate print in deep mud. Penetration through the substrate surface is shown in red. The hallux, which is not ‘reversed’ as in modern birds, leaves a posteromedially oriented entry furrow (**a**, **b**) as the digit plunges down and forward. The ankle is not immediately lifted during the stance phase, and as a result a metatarsal impression is created (**c**), elongating the track posteriorly. All digits converge beneath the surface and emerge together from the anterior end of the track (**d**).

Methods

Triassic theropod footprints. Fossil footprints, collected at 71° 24.88′ N, 22° 33.17′ W on the eastern slope of Wood Bjerg, Jameson Land, East Greenland, were mechanically prepared to remove infilled matrix. Four elongate prints were transversely or sagitally sectioned with a rotary rock saw at 5 mm intervals to trace the subsurface path of each toe and determine foot penetration angles. We assessed the mobility of the hallux in two specimens of *Coelophysis bauri* (Museum of Comparative Zoology 4334, American Museum of Natural History 7226) by mounting the digital elements forming the metatarsophalangeal and interphalangeal joints at the extremes of their excursion ranges as indicated by the geometry of the articular facets. Images of the maximal excursion ranges, taken in standard anatomical perspectives, were captured by a Toshiba Image Master CCD Color Camera mounted on a Nikon SMZ-2T binocular microscope, and printed on a Sony Mavigraph colour video printer. Three-dimensional reconstructions of foot movement were modelled (based on the pedal anatomy of *Coelophysis bauri*) and rendered using Alias/Wavefront Studio 8.5 on a Silicon Graphics Indigo^2 IMPACT computer. Foot positions were reconstructed on the basis of penetration angles, hallucal cleft orientations, metatarsal impression slopes and toe convergence preserved in deep Greenlandic tracks.

Avian footprints. We videotaped an adult female turkey (*Meleagris gallopavo*) and an adult male helmeted guineafowl (*Numida meleagris*) in simultaneous lateral and anterior/posterior views as they walked and ran across a clay-rich, sandy soil. The soil was variously hydrated to produce substrate consistencies ranging from a firm, plasticine-like surface, with a depth of 7 mm (Fig. 1g), to a highly compliant mud with a depth of 61 mm (Fig. 1j). Trackways and individual tracks were documented by stereophotography; some prints were cast in plaster.

Received 9 February; accepted 15 March 1999.

---

1. Hitchcock, E. *Ichnology of New England: A Report on the Sandstone of the Connecticut Valley, especially its Fossil Footmarks, made to the Government of the Commonwealth of Massachusetts* (W. White, Boston, 1858).

2. Lull, R. S. Triassic life of the Connecticut Valley. *Conn. State Geol. Nat. Hist. Surv. Bull.* **81,** 1–336 (1953).
3. Gillette, D. D. & Lockley, M. G. eds *Dinosaur Tracks and Traces* (Cambridge University Press, Cambridge, 1989).
4. Thulborn, T. *Dinosaur Tracks* (Chapman and Hall, London, 1990).
5. Lockley, M. G. *Tracking Dinosaurs: A New Look at an Ancient World* (Cambridge University Press, Cambridge, 1991).
6. Alexander, R. McN. Estimates of speeds of dinosaurs. *Nature* **261,** 129–130 (1976).
7. Coombs, W. P. Jr Swimming ability of carnivorous dinosaurs. *Science* **207,** 1198–1200 (1980).
8. Farlow, J. O. Estimates of dinosaur speeds from a new trackway site in Texas. *Nature* **294,** 747–748 (1981).
9. Thulborn, R. A. Speeds and gaits of dinosaurs. *Palaeogeogr. Palaeoclimatol. Palaeoecol.* **38,** 227–256 (1982).
10. Thulborn, R. A. & Wade, M. Dinosaur trackways in the Winton Formation (mid-Cretaceous) of Queensland. *Mem. Qd. Mus.* **21,** 413–517 (1984).
11. Padian, K. & Olsen, P. E. in *Dinosaur Tracks and Traces* (eds Gillette, D. D. & Lockley, M. G.) 231–241 (Cambridge University Press, Cambridge, 1989).
12. Jenkins, F. A. Jr *et al.* Late Triassic continental vertebrates and depositional environments of the Fleming Fjord Formation, Jameson Land, East Greenland. *Meddr. Grønland Geoscience* **32,** 1–25 (1994).
13. Clemmensen, L. B., Kent, D. V. & Jenkins, F. A. Jr A Late Triassic lake system in East Greenland: facies, depositional cycles and palaeoclimate. *Palaeogeogr. Palaeoclimatol. Palaeoecol.* **140,** 135–159 (1998).
14. Lull, R. S. Fossil footprints of the Jura-Trias of North America. *Mem. Bos. Soc. Nat. Hist.* **1904,** 461–557 (1904).
15. Olsen, P. E. & Galton, P. M. A review of the reptile and amphibian assemblages from the Stormberg of southern Africa, with special emphasis on the footprints and the age of the Stormberg. *Palaeont. Afr.* **25,** 87–110 (1984).
16. Olsen, P. E., Smith, J. B. & McDonald, N. G. Type material of the type species of the classic theropod footprint genera *Eubrontes*, *Anchisauripus*, and *Grallator* (Early Jurassic, Hartford and Deerfield Basins, Connecticut and Massachusetts, U.S.A.). *J. Vert. Paleo.* **18,** 586–601 (1998).
17. Baird, D. Triassic reptile footprint faunules from Milford, New Jersey. *Bull. Mus. Comp. Zool.* **117,** 449–520 (1957).
18. Sereno, P. C., Forster, C. A., Rogers, R. R. & Monetta, A. M. Primitive dinosaur skeleton from Argentina and the early evolution of Dinosauria. *Nature* **361,** 64–66 (1993).
19. Novas, F. E. New information on the systematics and postcranial skeleton of *Herrerasaurus ischigualastensis* (Theropoda: Herrerasauridae) from the Ischigualasto Formation (Upper Triassic) of Argentina. *J. Vert. Paleo.* **13,** 400–423 (1993).
20. Colbert, E. H. The Triassic dinosaur *Coelophysis*. *Mus. N. Ariz. Bull.* **57,** 1–160 (1989).
21. Raath, M. A. A new coelurosaurian dinosaur from the Forest Sandstone of Rhodesia. *Arnoldia* **4,** 1–25 (1969).
22. Sereno, P. C. & Wild, R. *Procompsognathus*: theropod, "thecodont" or both? *J. Vert. Paleo.* **12,** 435–458 (1992).
23. Camp, C. L. A new type of small bipedal dinosaur from the Navajo Sandstone of Arizona. *Univ. Cal. Pub. Geol. Sci.* **24,** 39–56 (1936).
24. Welles, S. P. *Dilophosaurus wetherilli* (Dinosauria, Theropoda) osteology and comparisons. *Palaeontogr. Abt. A* **185,** 85–180 (1984).
25. Nopcsa, F. On the origin of flight in birds. *Proc. Zool. Soc. Lond.* **1923,** 463–477 (1923).
26. Thulborn, R. A. The avian relationships of *Archaeopteryx*, and the origin of birds. *Zool. J. Linn. Soc.* **82,** 119–158 (1984).
27. Gauthier, J. Saurischian monophyly and the origin of birds. *Mem. Calif. Acad. Sci.* **8,** 1–55 (1986).
28. Gatesy, S. M. Hind limb movements of the American alligator (*Alligator mississippiensis*) and postural grades. *J. Zool. (Lond.)* **224,** 577–588 (1991).
29. Tarsitano, S. Stance and gait in theropod dinosaurs. *Acta Palaeontol. Pol.* **28,** 251–264 (1983).
30. Gatesy, S. M. Caudofemoral musculature and the evolution of theropod locomotion. *Paleobiology* **16,** 170–186 (1990).

Acknowledgements. We thank L. B. Clemmensen, the Danish Polar Center and the Commission for Scientific Research in Greenland for support of field work, L. L. Meszoly for rendering Fig. 1, M. A. Norell and A. R. Davidson for access to *Coelophysis bauri* (AMNH 7226), Alias/Wavefront for software support, and J. O. Farlow, J. R. Hutchinson, M. G. Lockley, P. E. Olsen, K. Padian, D. Norman and R. A. Thulborn for critical advice. This work was supported by grants from the National Science Foundation, the Carlsberg Foundation, and the Putnam Expeditionary Fund of Harvard University.

Correspondence should be addressed to S.M.G. (e-mail: Stephen_Gatesy@Brown.edu).

Evolution of genetic mechanisms controlling petal development

Elena M. Kramer & Vivian F. Irish

Department of Molecular, Cellular and Developmental Biology, Yale University, PO Box 208104, New Haven, Connecticut 06520–8104, USA

Molecular genetic studies in *Arabidopsis thaliana* and other higher-eudicot flowering plants have led to the development of the 'ABC' model of the determination of organ identity in flowers, in which three classes of gene, *A*, *B* and *C*, are thought to work together to determine organ identity[1,2]. According to this model, the *B*-class genes *APETALA3* (*AP3*) and *PISTILLATA* (*PI*) act to specify petal and stamen identity. Here we test whether the roles of these genes are conserved throughout the angiosperms by analysing the expression of *AP3* and *PI* orthologues in the lower eudicot subclass Ranunculidae. We show that, although expression of these orthologues in the stamens is conserved, the expression patterns in the petals differ from those found in the higher eudicots. The differences between these expression patterns suggest that the function of *AP3* and *PI* homologues as *B*-class organ-identity genes is not rigidly conserved among all angiosperms. These observations have important implications for understanding the evolution of both angiosperm petals and the genetic mechanisms that control the identities of floral organs.

The ABC model postulates that sepal identity is established by the functions of *A* genes alone, petals by *A* and *B*, stamens by *B* and *C*, and carpels by *C* function alone[1,2]. Orthologous genes from the three classes have been identified in *Arabidopsis* and *Antirrhinum*[1], and subsequently in a number of other species, including *Nicotiana tabacum* (tobacco), *Solanum tuberosum* (potato) and *Petunia hybrida* (reviewed in ref. 3). The expression patterns and, where examined, the function of these genes appear to be similar in all of the species analysed[3,4], leading to the suggestion that the ABC model is conserved throughout the angiosperms[5]. However, all of the species in which the *ABC* genes have been well analysed are members of a monophyletic clade known as the higher eudicots. Although this group contains the majority of angiosperm species, it does not represent the full range of the flowering plants.

To assess the extent of conservation of the ABC model, we have

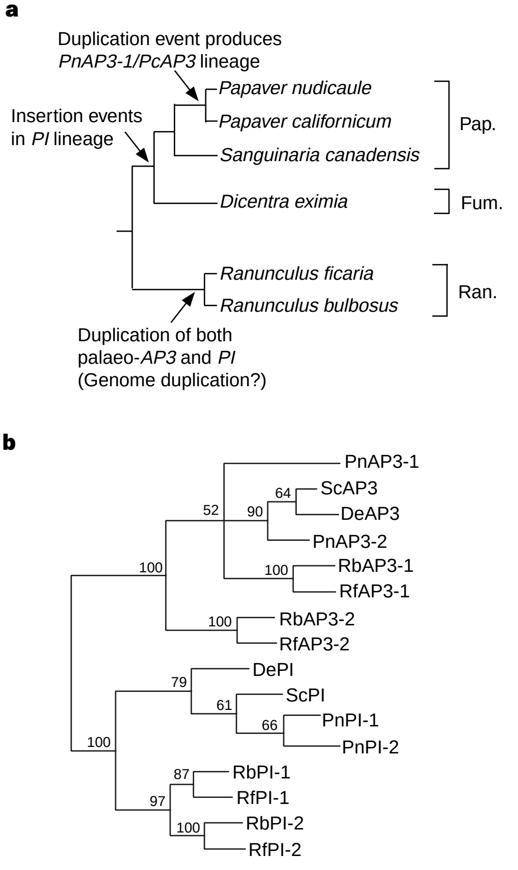

Figure 1 Gene and species phylogenies. **a**, Simplified phylogeny showing the relationships between Ranunculid species included in this study (based on ref. 22). Major events in the course of palaeo-*AP3* and *PI* gene evolution are shown. Pap.: Papaveraceae; Fum.: Fumariaceae; Ran.: Ranunculaceae. **b**, Gene tree of Ranunculid palaeo-*AP3* and *PI* lineage members based on parsimony analysis of nucleotide sequence. The numbers next to the nodes give bootstrap values from 1,000 replicates. A single tree of 1,839 steps was generated. Each cDNA was named using the first letter of the genus and species from which it was isolated followed by either *AP3* or *PI*, depending on its homology.